Supporting Information

Kastenhuber et al. 10.1073/pnas.1716483114

SI Materials and Methods

One sgRNA was cloned into the px330 vector, which was a gift from Feng Zhang (Addgene; plasmid 42230), and a second U6-sgRNA cassette was inserted into the XbaI site with XbaI-NheI overhangs. As indicated, for other experiments (Fig. S1), the lenti-CRISPR vector was a gift from David Sabatini (Addgene; plasmid 70662). The pT3 transposon and SBase vectors were a kind gift of Xin Chen, University of California, San Francisco, CA.

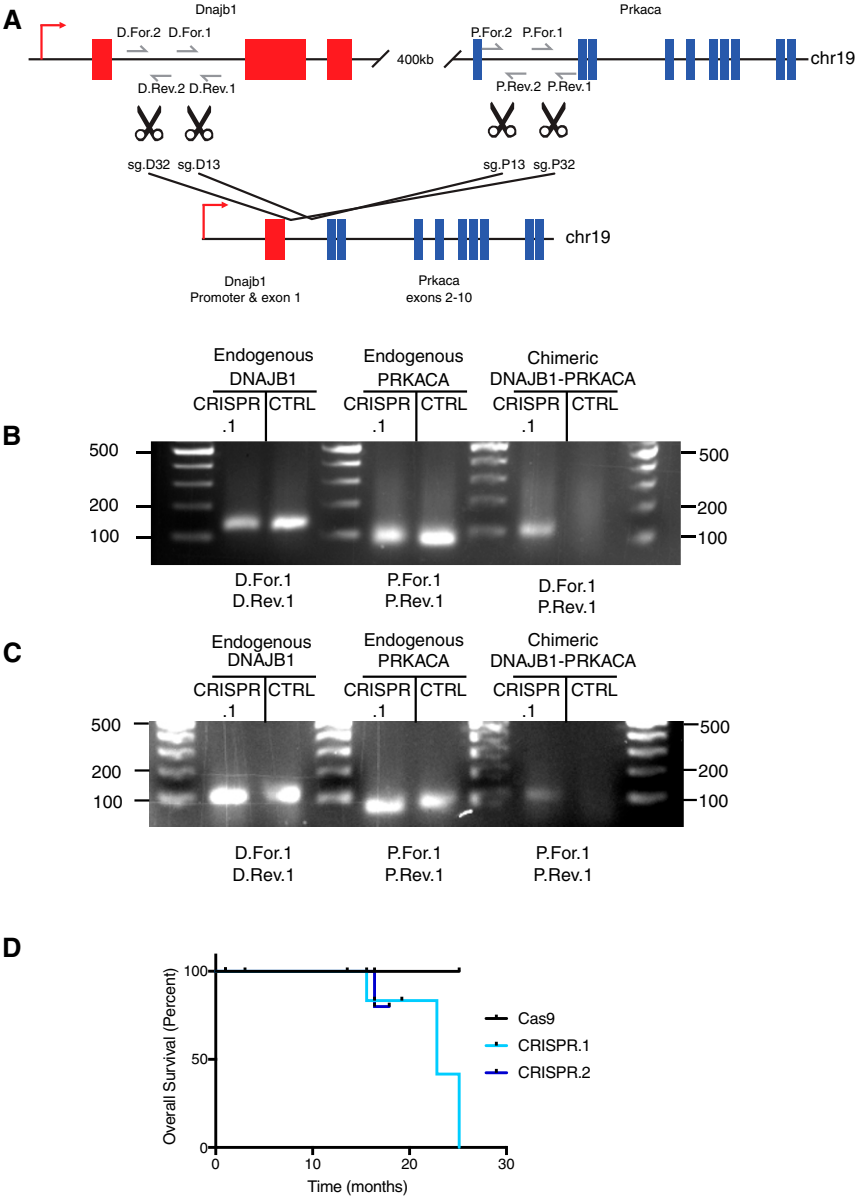

Fig. S1. Validation of CRISPR-mediated deletion. (*A*) Schematic of sgRNAs and primers. (*B*) Detection of genomic deletion in NIH 3T3 cells infected with a tandem guide lentiCRISPR construct. (*C*) Detection of deletion in genomic DNA extracts from whole livers 4 d following hydrodynamic tail-vein injection of the same construct. (*D*) Overall survival of mice following hydrodynamic tail-vein injection of the lentiCRISPR plasmid DNA.

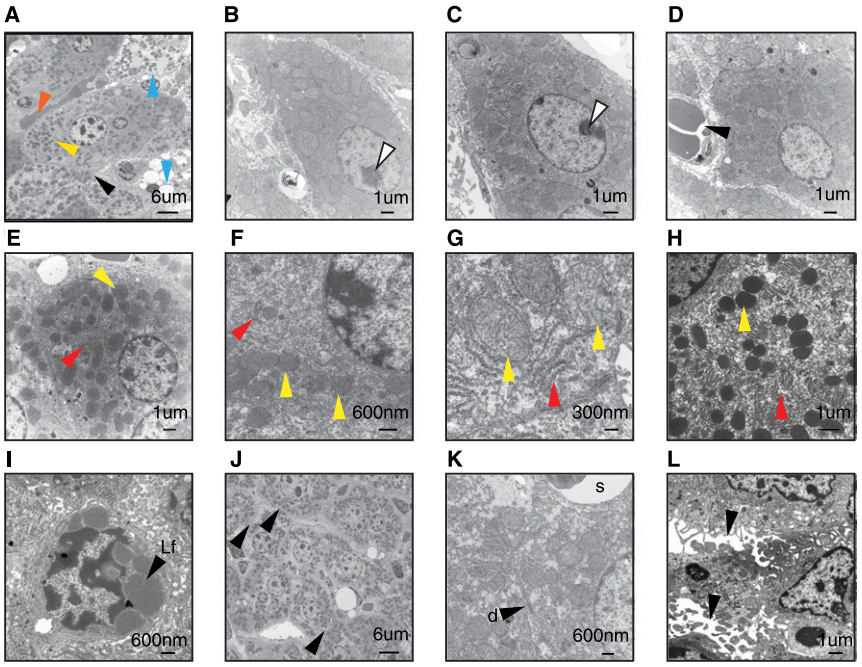

Fig. S2. Additional ultrastructural analysis of murine FL-HCC. (*A*) Higher magnification of Fig. 3*A*. FL-HCC tumor cells are enlarged with abnormally abundant mitochondria (yellow arrowhead). Necrotic cells (blue), nonfenestrated vessels (orange), and indistinct cell–cell junctions (black). (*B* and *C*) Tumor nuclei are large and round-to-indented with prominent nucleoli (white). (*D*) Tumor-associated vasculature (black). (*E–H*) Abundant mitochondria (yellow) surrounded by rough endoplasmic reticulum (red) with scant smooth endoplasmic reticulum. (*I*) Lipofuscin (Lf). (*J*) Simple, indistinct cell–cell junctions (black). (*K*) Rare desmosome (d) with nearby sinusoid (s). (*L*) Bile canniculi are sometimes widened (black).

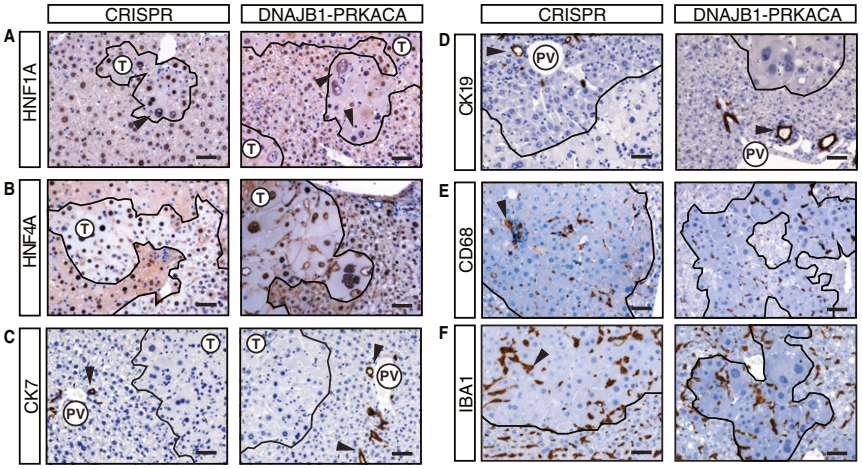

Fig. S3. Additional molecular characterization of murine FL-HCC. Indicated genotypes stained for hepatocyte markers (*A*) HNF1A and (*B*) HNF4A (arrowheads indicate tumor cells with reduced staining), cholangiocyte markers (*C*) CK7 and (*D*) CK19 (arrowheads indicate bile ducts; PV, portal vein), (*E*) CD68 (arrowheads indicate CD68+ infiltrating macrophages), and (*F*) IBA1 confirming *E* (arrowheads indicate IBA1+ infiltrating macrophages). (Scale bars, 50 μm.)

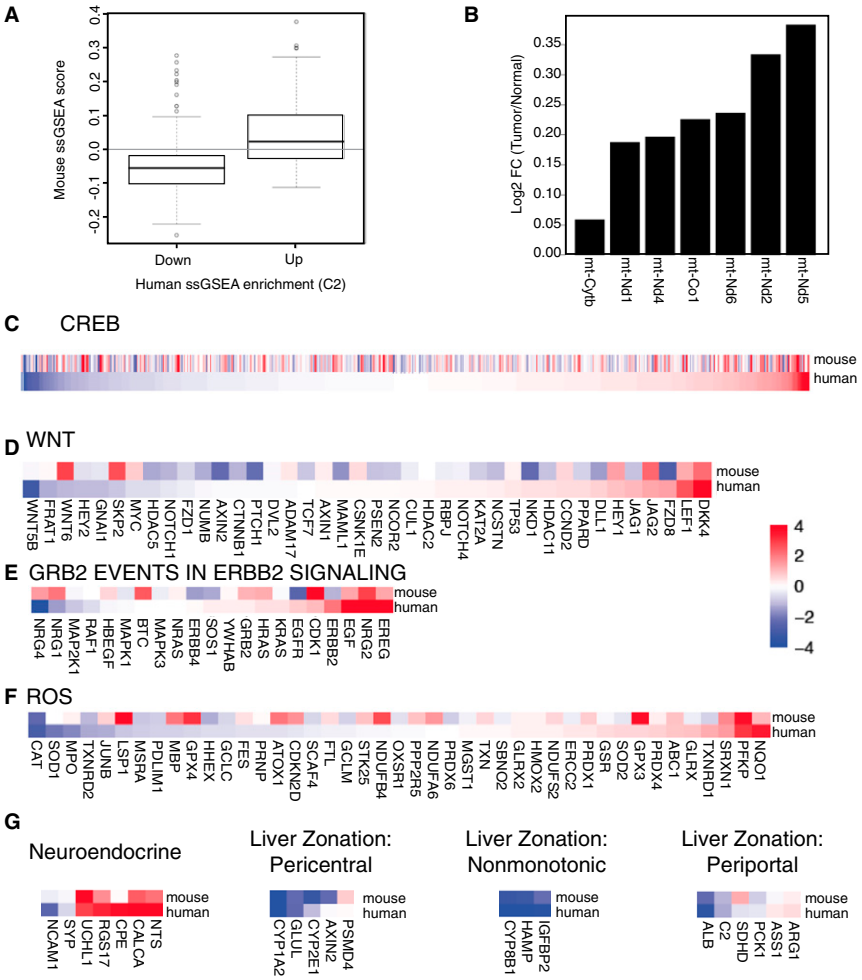

Fig. S4. Gene expression of FL-HCC–associated gene sets of interest. (*A*) ssGSEA enrichment scores from mouse tumor differential expression for gene sets significantly enriched in either up-regulated or down-regulated human gene expression data (30) ($P = 4.22 \times 10^{-17}$). (*B*) Gene expression for genes encoded by mitochondrial DNA. (*C*–*F*) Gene expression of corresponding mouse and human (30) genes in the specified gene sets: (*C*) CREB targets; (*D*) Wnt signaling pathway; (*E*) GRB2 events in ERBB2 signaling; and (*F*) genes up-regulated by ROS. (*G*) Lineage-specific genes including neuroendocrine markers (30) and liver zone-specific genes (34).

A

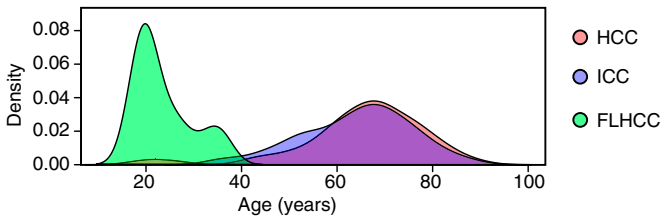

B

Age	Gender	Mutations	CNA	Survival Status	Survival (months)
18	Male	DNAJB1-PRKACA, APC, CHEK2	$TERT^{AMP}$	Alive	29
18	Male	DNAJB1-PRKACA, CTNNB1	none	Alive	15
21	Female	DNAJB1-PRKACA, CTNNB1 LOC101928035-ZFHX3, ATR (met only)	$SOX17^{AMP}$ (Met only)	Alive, Brain Metastasis	31

C

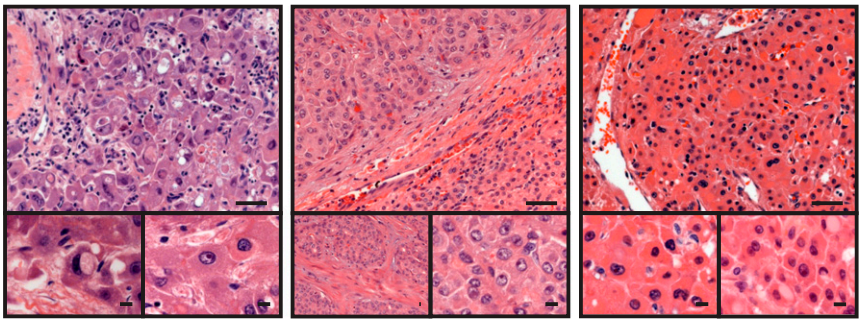

Fig. S5. Wnt pathway alteration in human FL-HCC. (*A*) Age distribution of patients with the indicated types of liver tumors (HCC, $n = 129$; ICC, $n = 165$; FL-HCC, $n = 16$). (*B*) Clinical and genomic characteristics of three cases of FL-HCC with Wnt pathway mutation. (*C*) H&E staining reveals classic FL-HCC morphology in cases with Wnt pathway mutations. [Scale bars, 50 μm (*Top*) and 10 μm (*Bottom*).]

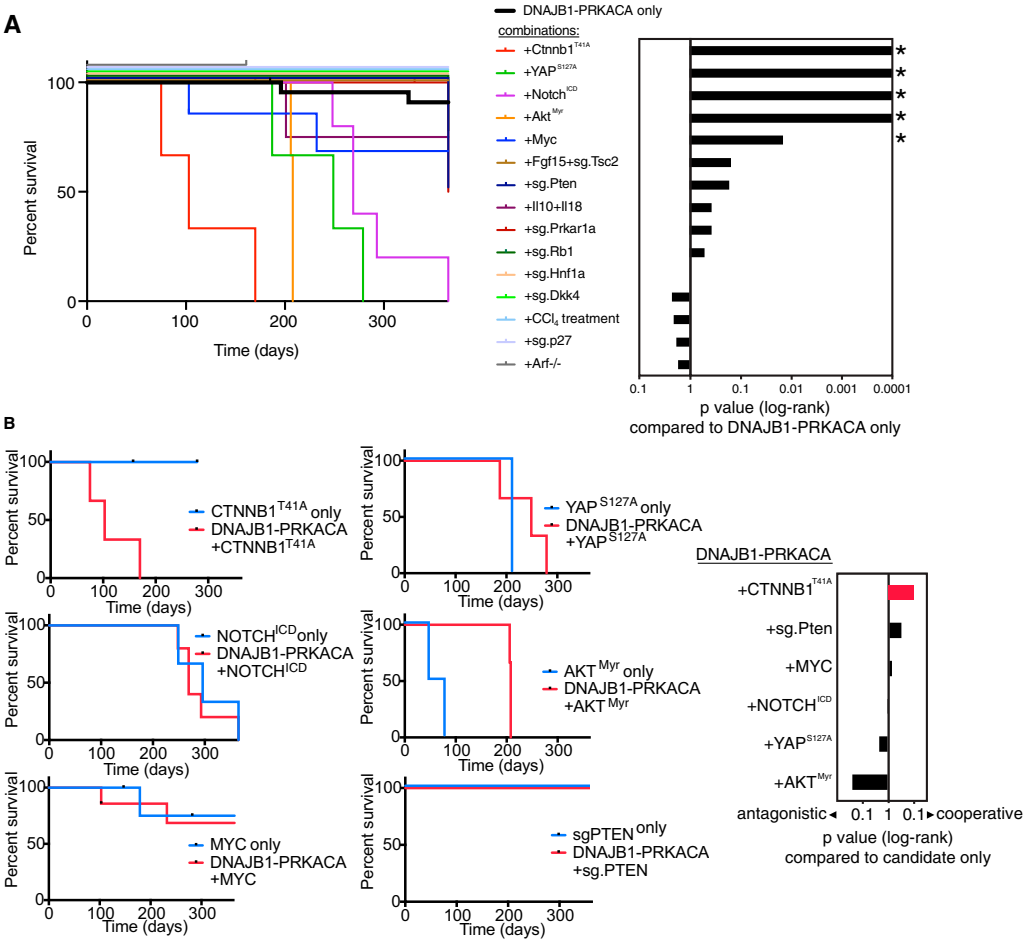

Fig. S6. Screen for cooperating mutations. (*A*) Survival data of cohorts injected with DNAJB1–PRKACA fusion cDNA alone or in combination with the indicated genotypes. *Log-rank $P < 0.01$. (*B*) Survival data of cohorts injected with candidate genes from *A* alone or in combination with the fusion. CTNNB1^{T41A} cooperates with DNAJB1–PRKACA, resulting in higher lethality than either gene alone.

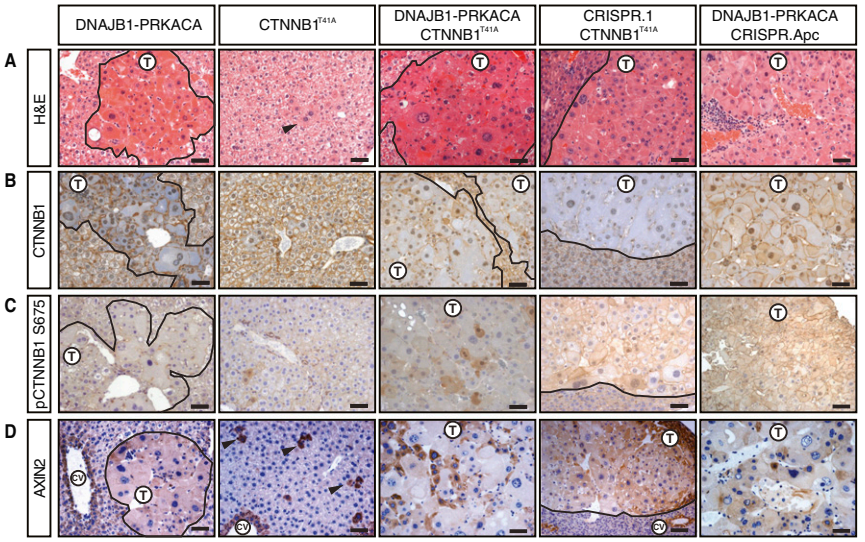

Fig. S7. Wnt pathway in murine FL-HCC. Livers injected with *DNAJB1–PRKACA*, *CTNNB1*^{T41A}, *DNAJB1–PRKACA* + *CTNNB1*^{T41A}, CRISPR.1 + *CTNNB1*^{T41A}, or *DNAJB1–PRKACA* + CRISPR.Apc. (*A*) H&E or immunohistochemistry with antibodies against (*B*) CTNNB1, (*C*) p-CTNNB1 S675 (PKA target site), and (*D*) AXIN2 (Wnt target gene). CV, central vein (AXIN2 internal positive control). Arrowheads, atypical hepatocytes; T, tumor. (Scale bars, 50 μm.)

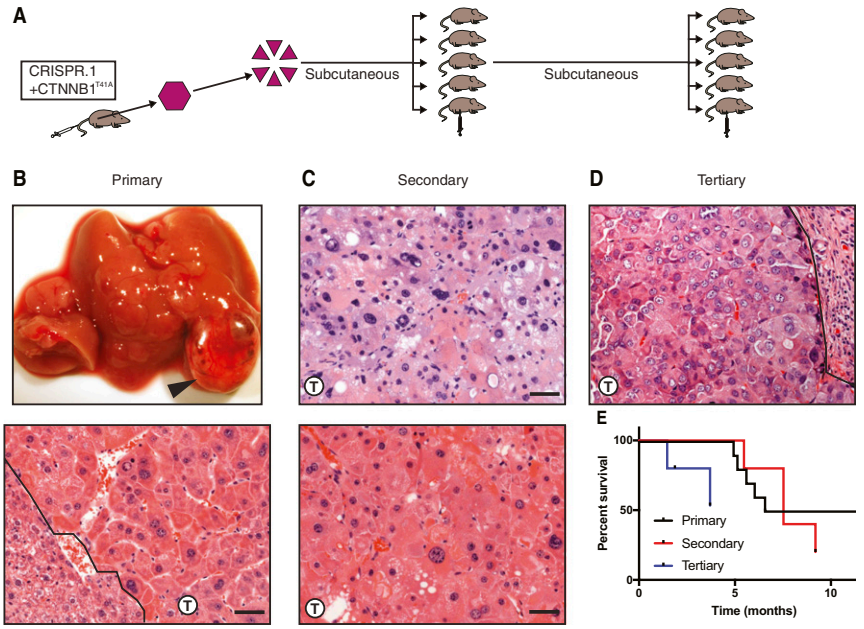

Fig. S8. Serial transplantation of murine FL-HCC. (*A*) Primary tumor driven by CRISPR.1 fusion; CTNNB1^{T41A} was minced and transplanted s.c. into syngeneic C57BL6 mice. (*B–D*) Macroscopic view (*Top*) and histology (*Bottom*) of primary tumor (arrowhead) (*B*), transplanted tumors (secondary) from two independent recipients (*Top* and *Bottom*) (*C*), and second serial transplantation of a tumor from Fig. S7*C* (tertiary) (*D*). (*E*) Survival of cohorts of primary tumors (from Fig. 5*C*) and tumors from two rounds of serial transplantation. (Scale bars, 50 μm.)

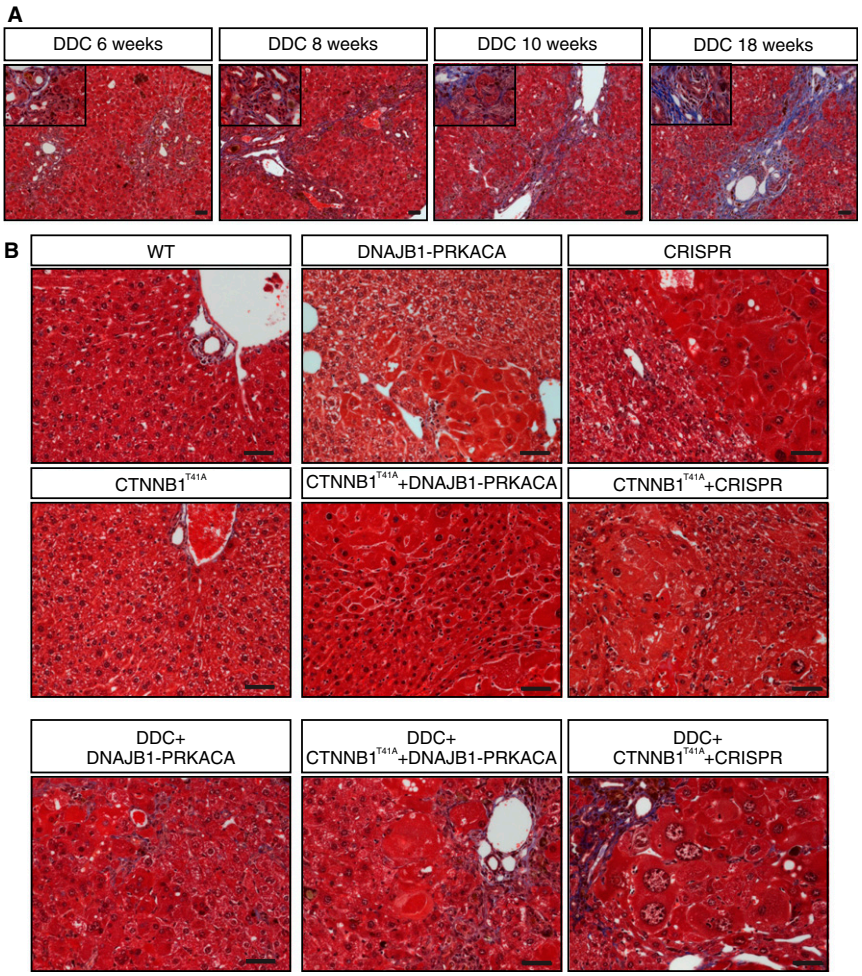

Fig. S9. DDC-induced changes in liver pathology. (*A*) Masson's trichrome staining indicating progressive development of fibrosis and atypical ductal proliferation (*Insets*). (Scale bars, 50 μm.) (*B*) No indication of fibrosis was detected in mice with any combination of genetic perturbations when the mice were fed a normal diet. Mild fibrosis stained positive (blue) in some areas adjacent to tumors following DDC treatment and injection with the indicated constructs. (Scale bars, 50 μm.)

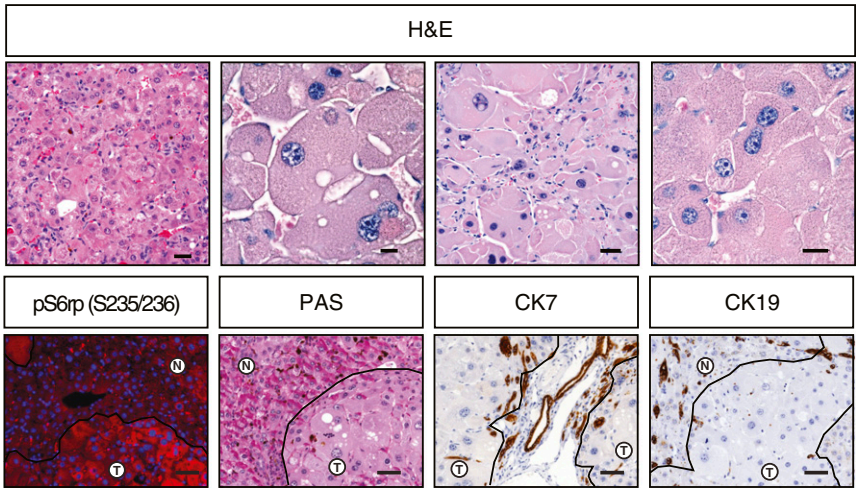

Fig. S10. Stable phenotype in DDC-treated tumors. The indicated histological features were found in tumors expressing *DNAJB1–PRKACA* and *CTNNB1*^{T41A} in DDC-treated mice (*Top*). Tumors had (from left to right) recognizable inflammation, pale bodies, atypical nuclei, and abundant rough endoplasmic reticulum. (Scale bars, 25 μm.) *DNAJB1–PRKACA*/*CTNNB1*^{T41A}/DDC tumors were pS6rp$^{S235/236}$+, PAS−, CK7−, and CK19− (*Bottom*). (Scale bars, 50 μm.)

Table S1. Sequences for sgRNAs and primers

Name	Description	Sequence, 5′–3′
sg.Dnajb1.1	Mouse CRISPR	TGACAACATATTCGGTAGTA
sg.Dnajb1.2	Mouse CRISPR	CTGGTCGCACCGAGATCTAG
sg.Prkaca.1	Mouse CRISPR	GAGAGGGGAACGGTATCCT
sg.Prkaca.2	Mouse CRISPR	TTCAGTCCCAATCGAGTGC
Dnajb1.For	Mouse gDNA primer	GGAGGATGGAGCAGTCACG
Dnajb1.Rev	Mouse gDNA primer	CCCAATGGCAATAGGAGC
Prkaca.For.1	Mouse gDNA primer	GCAAGGTTTGACGGAGG
Prkaca.Rev.1	Mouse gDNA primer	CATTTGGTTCTGTCTTGTTCC
Prkaca.For.2	Mouse gDNA primer	GTGGGATTCGTTACAGTGGC
Prkaca.Rev.2	Mouse gDNA primer	TGCGGACTGAAGACCACC
RT.mmDnajb1.For8	Mouse RT primer	ACCGCTATGGAGAGGAAGTG
RT.mmPrkaca.Rev8	Mouse RT primer	GGCTGTATTCTGAGAAGGGGT

Dataset S1. Murine FL-HCC differential gene expression

Dataset S1

RNA-seq of murine tumors and normal liver.

Dataset S2. Murine FL-HCC gene set enrichment analysis

Dataset S2

GSEA analysis of functionally annotated gene sets based on Dataset S1.